RESEARCH PAPER

PCCP
www.rsc.org/pccp

Cross-sections for the $H + H_2O \rightarrow OH + H_2$ and $H + D_2O \rightarrow OD + HD$ abstraction reactions†

M. Brouard,*[a] S. Marinakis,[a] L. Rubio Lago,[a] F. Quadrini,[a] D. Solaiman,[a] C. Vallance,[a] F. J. Aoiz,[b] L. Bañares[b] and J. F. Castillo[b]

[a] *The Department of Chemistry, The Physical and Theoretical Chemistry Laboratory, University of Oxford, South Parks Road, Oxford, UK OX1 3QZ. E-mail: mark.brouard@chemistry.ox.ac.uk*

[b] *Departamento de Química Física, Facultad de Química, Universidad Complutense 28040 Madrid, Spain*

Received 25th June 2004, Accepted 6th August 2004
First published as an Advance Article on the web 26th August 2004

Absolute values of the cross-section for the abstraction reaction between fast H atoms and D_2O have been determined experimentally at mean collision energies of 1.83 eV and 2.48 eV. The data support the value for the cross-section recently reported for the $H + H_2O$ reaction at 2.46 eV, which was significantly lower than previous measurements. The measurements employ the photodissociation of water as a calibrant for OH(OD) concentration. The OH rotational quantum state population distributions for the fully protonated reaction, as well as those for the photodissociation of water, are shown to be in good agreement with previous work. The measurements are compared with new quasi-classical trajectory calculations and published quantum mechanical scattering calculations using the most recently developed potential energy surface.

1. Introduction

The abstraction and exchange reactions between H atoms and water have played a key role in the development of our understanding of reaction dynamics.[1–8] The abstraction reaction is important in influencing the overall rate of combustion of hydrogen and oxygen,[9] and as a result has been the subject of numerous kinetic studies.[10] The mechanism of the reaction has also been the subject of much attention.[1–8] It is the simplest reaction in which the dynamics can be influenced by both the kinetic energy of the reactants and the excitation of different vibrational modes of the polyatomic reactant.[6] Because the reactions involve three light atoms, high level theory can be used to probe the dynamics and, consequently, studies of this system have been central to the development of a quantitative understanding of polyatomic chemical reactions.[1,2,4,7]

One vital test of theory is provided by the absolute reaction cross-section. However, the necessity of determining absolute product OH or H_2 number densities makes this a difficult quantity to measure accurately. Pioneering work by Wolfrum and Kleinermanns and coworkers[11–16] overcame this problem by calibrating the OH product number density relative to that generated photolytically from a precursor with a known photodissociation cross-section. The experimental data of Wolfrum and coworkers for both the abstraction and exchange reaction cross-sections have been collated recently in ref. 17. However, the cross-sections they obtained for the $H + H_2O$ and $H + D_2O$ abstraction reactions[11–16] are significantly larger than current theoretical estimates,[7,18,19] and a redetermination is therefore timely. Interestingly, the experimental cross-sections for the exchange reactions, which employ different calibrants, are in much better agreement with theory.[18]

In spite of the apparent simplicity of the reaction, the theoretical and computational tasks involved in calculating the total reaction cross-section are challenging, particularly at the high energies typically accessed in hot H/D atom experiments. Chemical accuracy in the potential energy surface (PES), which demands a very high level of *ab initio* electronic structure calculation, is required over a broad range of molecular configurations. Nevertheless, the two most recently developed PESs, those by Schatz and coworkers,[20] known as the WSLFH PES, and by Collins and coworkers,[21,22] known as the YZCL2 PES, represent significant advances, and would appear to approach the accuracy necessary for reliable, high energy dynamical studies.

The dynamical calculations are also highly demanding. The majority of work has involved using the quasi-classical trajectory (QCT) approach.[1,4,7,23,24] However, because the abstraction reaction probability is very low, QCT studies must employ large ensembles of trajectories, making such calculations computationally quite expensive. Previously, quantum mechanical (QM) scattering methods could only be applied to the reaction if approximations were made, either by reducing the dimensionality of the calculation, or by treating the angular momentum approximately. More recently, however, it has been possible to test rigorously the approximations employed.[18,19,25,26] For example, full dimensionality QM scattering calculations for total angular momentum $J = 0$ and $J = 15$ have now been performed up to a collision energy of 1.6 eV, and these indicate that the OH bond can be treated satisfactorily as a spectator for the abstraction reaction, but not for exchange.[25]

Recently, we presented a new determination of the cross-section for the $H + H_2O$ abstraction reaction, and of the OH product rotational quantum state populations, at a mean collision energy of 2.46 eV.[27] These data were compared with the results from five-dimensional (5D) QM and six-dimensional (6D) QCT calculations. In spite of the computational difficulties described above, experiment and theory were shown to agree for the abstraction reaction cross-section to within a factor of two.[27] The 5D QM calculations employed the YZCL2 PES,[21,22] determined using the iterative procedures developed

† This paper was written as part of the EC Research Training Network on Reaction Dynamics (HPRN-CT-1999-00007).

DOI: 10.1039/b409667c

by Collins and coworkers,[28] which appears to be the most accurate global PES available at present.[18,24,29] The 5D QM scattering calculations treated one OH bond as a spectator, and employed the initial state-selected time-dependent wave packet approach to state-to-state integral cross-sections for four-atom reactions developed recently by Zhang and coworkers.[19] For partial waves with $J > 0$ the calculations were performed without using the centrifugal sudden (CS) approximation, which has been shown recently to be unreliable for these reactions.[26]

In the present paper, we extend our previous work on the abstraction reaction

$$H + H_2O \rightarrow OH + H_2 \quad (1)$$

to determination of cross-sections for the isotopic reaction

$$H + D_2O \rightarrow OD + HD, \quad (2)$$

at mean collision energies close to 1.8 eV and 2.5 eV. Our previous experiments on the $H + H_2O$ abstraction reaction are also described more fully. The new determination of the cross-section for the deuterated reaction has been made by calibration of the OD product yield relative to the OD signals generated in the simultaneous photodissociation of mixtures of H_2O, D_2O, and HOD. The new results for $H + D_2O$ are therefore independent of our previous estimate of the cross-section for the $H + H_2O$ abstraction reaction, and are not based on a determination of the relative OH and OD yields from reactions (1) and (2). The experimental data are compared with the results of new QCT calculations for the deuterated reaction. In Section II we present details of the experimental and data analysis methods employed. Theoretical aspects of the present work are outlined in Section IIC, and the results are presented in Section III. In Section IV we compare the experimental data with the new theoretical calculations, and also discuss some of the potential limitations of the present experimental and theoretical work. Section V summarizes our main conclusions.

II. Method

A. Experimental

The method used to determine the $H + H_2O$ reaction cross-section has been described briefly in our previous paper.[27] Here we provide more details, particularly highlighting the slightly different procedures used to measure the $H + D_2O$ reaction cross-section. We employed the calibration technique of Wolfrum and Kleinermanns.[11] However, as with our previous work[27] we have used the *in situ* photodissociation of the target H_2O (HOD/D_2O) molecule itself as an 'internal' OH (OD) calibrant. This contrasts with the work of Wolfrum[11–15] and Kleinermanns[16] and coworkers, who used H_2O_2 or HNO_3 as calibrants, and performed the H-atom reaction and calibration experiments consecutively. In the present study, the OH (OD) products arise from two sources, one from photolysis of water at 193 nm, and the other from bimolecular reaction. The unravelling of these contributions is the key to the present cross-section measurements.

The experiments employed the laser pump–probe method. For the $H + H_2O$ reaction HBr was photolyzed with excimer laser radiation at 193 nm to generate fast H atoms, providing a mean collision energy of 2.46 eV with a full-width-at-half-maximum (FWHM) of 0.2 eV. The OH products were probed after a short time delay by laser induced fluorescence (LIF). For both the photolysis of H_2O and the $H + H_2O$ abstraction reaction, only OH fragments born in the $v' = 0$ vibrational level could be observed. LIF spectra in the region of the R↑ branch head of the 0–0 band of the OH A ← X transition were recorded as a function of time delay, $\Delta\tau$, and HBr concentration, [HBr]. $\Delta\tau$ was varied between 50 ns and 150 ns, and total pressures, p, (of varying HBr : H_2O composition) were maintained between 100 mTorr and 200 mTorr. Fluorescence signals were sent to a boxcar integrator prior to transferral to a PC, where the signal was averaged typically over 20 laser shots at each wavelength step.

In the case of the $H + D_2O$ reaction, the procedures were slightly different. Radiation of 193 nm was used to photodissociate either HBr or HCl to generate fast excited H atoms, yielding mean collision energies $\langle E_t \rangle = 2.48$ eV and $\langle E_t \rangle = 1.83$ eV, respectively. The partial pressure ratio of photolysis precursor to reactant water molecule was maintained at 50 : 50 for the 2.48 eV measurements, and 75 : 25 for the 1.83 eV experiments. The latter ratio was used to reduce somewhat the contribution to the signal from photolysis of water. The 2.48 eV measurements were made at a time delay of 50 ns, while for those at 1.83 eV the time delay was varied between the values of $\Delta\tau = 50$ ns to $\Delta\tau = 1$ μs (see following Section). In both cases, the total pressure was maintained at $p \leq 100$ mTorr. The experiments were performed using equilibrated mixtures of H_2O, HOD, and D_2O, and, therefore, both OH and OD LIF signals were observed in these experiments.

Relative transition intensities were extracted by fitting Gaussian line-functions to the assigned experimental spectra. Representative OH/OD LIF spectra obtained in the study of the $H + D_2O$ reaction are shown in Fig. 1. Assignments were made using the output from the program LIFBASE.[30] The method used to analyze the OH and OD relative population data obtained from the LIF spectra is explained in detail in Section IIB.

For both reactive systems, scans with only HCl or HBr flowing through the chamber were run regularly prior to the reaction cross-section measurements to ensure that there were no signals from the reaction of H atoms with background molecular oxygen in the system. To ensure that unwanted, surface-catalyzed side reactions in the gas lines did not interfere with the measurements, the two separate gas inlets were made from teflon tubing. In order to avoid H reagent atom fly-out from the detection region, the probe beam diameter used was larger than that of the pump. In this way, all of the OH/OD produced at a given pump–probe delay time were probed. Experiments were also performed to check that at 50 ns time delays, the OH/OD signals increased linearly with HX concentration, until quenching of the LIF signal by the precursor became important. A linear increase in signal with HX concentration is in accord with the analysis described below, and also supports the view that loss of reactants through dark reactions (such as wall catalyzed reaction between precursor and target molecule) did not occur to a significant extent. Finally, we have also performed some spectral scans of individual OH/OD transitions with Doppler resolution.

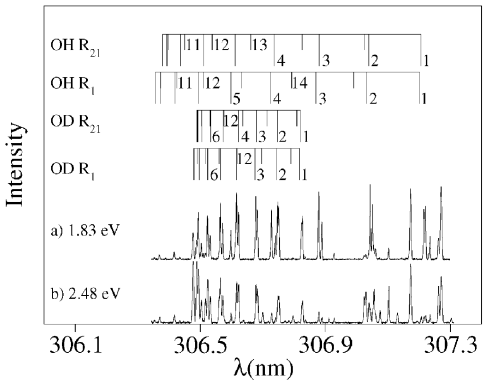

Fig. 1 Example OD LIF spectra recorded to measure the $H + D_2O$ abstraction reaction cros-ssection. The experiments were conducted with time delays of 50 ns and total pressures of 100 mTorr at mean collision energies of (a) 1.83 eV and (b) 2.48 eV. Spectral assignments have been made using the program LIFBASE.[30]

Photodissociation of water yields sharper, narrower line-profiles than reaction, and thus the width of the features provides a further check on the fraction of the signal arising from reaction. These data again support the analysis described in the next subsection.

B. Analysis

The data analysis followed that described previously for the H + H_2O reaction.[27] At the short pump–probe time delays employed, the *relative* signal from bimolecular reaction, x (*i.e.* the LIF signal from reaction divided by the signal from photolysis), can be written[11]

$$x = a_{OH}\Delta\tau[HBr] \quad (3)$$

where the constant a_{OH} is given by

$$a_{OH} = \left(\frac{\sigma_{HBr}}{\sigma_{H_2O}}\right) v_{rel}\sigma_r.$$

σ_r is the abstraction reaction cross-section of interest, v_{rel} is the relative velocity, and the term in brackets is the ratio of photodissociation cross-sections for HBr[31–33] and H_2O[33–36] at 193 nm. These cross-sections are known quite precisely.[31–36] Here we use the current IUPAC recommended values (σ_{HBr} = (1.79 ± 0.36) × 10^{-18} cm^2, and σ_{H_2O} = (1.75 ± 0.26) × 10^{-21} cm^2,[33]) unless otherwise stated. We have made our own measurements of both absorption cross-sections that agree with the literature values to within 20%, although that for water was determined with significantly less precision than can be found in the literature. Note, that these measurements were performed under similar conditions to those in which the reaction cross-sections were measured, and therefore they provide confirmation that the purity of the reagents is maintained in the interaction region.

Because the rotational distribution obtained from the photolysis of water at 193 nm, $P_{ph}(N')$, is very cold[37,44] compared with that generated by reaction (1) at 2.5 eV,[12] the relative yield of OH from reaction, x, and the reactive population distribution, $P_r(N')$, could be determined by fitting the observed rotational population distributions, $P_{obs}(N')$, using the equation

$$P_{obs,R}(N') = fP_{r,R}(N') + (1 - f)P_{ph,R}(N'), \quad (4)$$

where N' is the total OH angular momentum quantum number apart from electron spin, and $f = x/(1 + x)$ is the fraction of the signal arising from reaction. Here the subscript R has been added to denote the fact that we have only used population data obtained on R↑ transitions (see further below). A global fit to over 30 separate population distributions was performed, in which the photodissociation populations, $P_{ph,R}(N')$, were constrained to the values determined in scans without HBr present, and the parameter a_{OH} in eqn. (3) and the reaction populations $P_{r,R}(N')$ were optimized. Although the results presented here are for the global fit to the entire data set, it is important to emphasize that separate analysis of the experimental data obtained at small and large values of $p \times \Delta\tau$ yield very similar reaction cross-sections, well within the experimental uncertainties quoted here (see also Section IV). A particular advantage of this procedure for extracting the reaction cross-section, rather than using a comparison of LIF intensities with and without photolysis precursor present, is that it is insensitive to changes in electronic quenching of OH that arise when the gas composition is changed.

The analysis in the case of H + D_2O was more complex, since a greater number of competing processes contribute to the LIF signal. In determining integral cross-sections from the spectra, isotopic exchange in the D_2O samples had to be taken carefully into account. The analysis assumed that the following equilibrium was established at the time the reaction was studied:

$$D_2O + H_2O \leftrightharpoons 2HOD$$

Under these conditions the photodissociation processes contributing to the OH and OD signals were

$$\begin{aligned} &H_2O + h\nu \rightarrow H + OH \quad \sigma_{H_2O} \\ &DOH + h\nu \rightarrow D + OH \quad \sigma_{DHO} \\ &HOD + h\nu \rightarrow H + OD \quad \sigma_{HOD} \\ &D_2O + h\nu \rightarrow D + OD \quad \sigma_{D_2O}, \end{aligned}$$

where we have also defined the relevant photodissociation cross-sections. The reactive contributions to the OH and OD signals, with H-atom photolysis precursor present, were

$$\begin{aligned} &H + H_2O \rightarrow HH + OH \quad \sigma_{HHOH} \\ &H + DOH \rightarrow HD + OH \quad \sigma_{HDOH} \\ &H + HOD \rightarrow HH + OD \quad \sigma_{HHOD} \\ &H + D_2O \rightarrow HD + OD \quad \sigma_{HDOD}. \end{aligned} \quad (5)$$

Because of the likelihood of day to day variations in the extent of isotopic exchange, a 'water only' spectrum was recorded prior to each scan made to determine the abstraction reaction cross-section. For the photolysis only processes, the relative OD to OH yields, Y, determined from fits to the raw spectra, after correction for the different Einstein absorption coefficients[30] and summed over all product quantum states, may be written

$$\frac{Y_{ph}^{OD}}{Y_{ph}^{OH}} = \frac{\sigma_{D_2O}\chi_{D_2O} + \sigma_{HOD}\chi_{HOD}}{\sigma_{H_2O}\chi_{H_2O} + \sigma_{DOH}\chi_{HOD}}.$$

The mole fractions, χ_i, of H_2O, D_2O, and HOD could thus be calculated using the relative photodissociation cross-sections measured by Nesbitt and coworkers,[37,38] together with the equilibrium constant (K_χ = 3.82 ± 0.05 at 22.4 °C),[39] where

$$K_\chi = \frac{\chi_{HOD}^2}{\chi_{D_2O}\chi_{H_2O}}.$$

For the majority of the experiments, χ_{D_2O} values ranging from 0.80 to 0.95 were determined, which were in reasonable, although not exact, agreement with the mole fractions expected based on the equilibrium water mixtures employed, due to isotopic exchange. Because $\sigma_{HOD} \simeq 25\sigma_{D_2O}$,[38] under these conditions the majority of the OD photolysis signal originates from HOD. The photodissociation cross-section data employed in the present study is further discussed in Section III.

With both water and photolysis precursor (HX, with X = Br or Cl) present, the ratio of reactive to photolytic OD signals can be written (analogous to eqn. (3))

$$x_{OD} = a_{OD}\Delta\tau[HX], \quad (6)$$

with

$$a_{OD} = \left(\frac{\sigma_{HDOD}\chi_{D_2O} + \sigma_{HHOD}\chi_{HOD}}{\sigma_{D_2O}\chi_{D_2O} + \sigma_{HOD}\chi_{HOD}}\right)\sigma_{HX}v_{rel}.$$

We employed the absorption cross-section of HCl at 193 nm recently determined by Lee and coworkers σ_{HCl} = (9.10 ± 0.05) × 10^{-20} cm^2,[40] which is close to the current IUPAC recommendation of 9.5 × 10^{-20} cm^2.[33] In principle, by varying the isotopic composition it would be possible to determine independently the cross-sections for the OD generating reactions (2) and (5). However, here we have used the reaction cross-section ratio determined by Zare and coworkers, $\sigma_{HHOD}/\sigma_{HDOD}$ = 1.27 ± 0.11[41] determined at a collision energy of 1.5 eV. The present analysis therefore assumes that this ratio doesn't differ significantly from unity as the collision energy is raised to 2.5 eV, which seems reasonable based on simple kinetic isotope arguments. Because the majority of the experiments employed reaction mixtures composed mainly of D_2O,

the returned H + D_2O reaction cross-section was found to be fairly insensitive to the ratio of cross-sections $\sigma_{HHOD}/\sigma_{HDOD}$. For example, a factor of two increase in the assumed value of the relative cross-section for the H + HOD reaction was found to lead to only a 20% decrease in the returned cross-section for the H + D_2O reaction.

Fits to the population data were achieved as described above for the H + H_2O reaction, using eqn. (4) with the cross-section for reaction (2), σ_{HDOD}, used as an adjustable parameter. Unlike for the H + H_2O experiments, for the H + D_2O studies at both collision energies the reactive OD rotational quantum state populations were constrained to those obtained previously.[14,15,24,41,42] For the experiments at 2.5 eV, the population data were taken from either our own work[24] or that of Wolfrum and coworkers.[14] The reactive signals at these collision energies are sufficiently large to ensure that the conditions may be adjusted to ensure that the reactive signal dominates over photodissociation of water. For the experiments performed at 1.83 eV, at which no previous work has been performed on the H + D_2O reaction, the population data were interpolated between that taken at around 1.5 eV[41,42] and that obtained between 2.2 eV and 2.5 eV.[14,15,24] The changes in OD rotational populations with increasing collision energy are quite modest, and this procedure introduces little uncertainty. A further complication with the 1.83 eV experiments is that the data taken at the shortest time delays (50 ns) suffered from a particularly large photolysis contribution to the recorded signal. For this reason time delays in the range 50 ns to 250 ns were employed, and the population data extrapolated to short times to minimize the effects of translational cooling of the H atoms.

In both sets of experiments population data were derived exclusively from R↑ branch LIF transitions of OH and OD. Because the P/R↑ and Q↑ branches probe separately the OH/OD A′ and A″ λ-doublet levels, it was necessary to account for differences in the λ-doublet population propensities observed for reaction and photolysis. For example, the reaction populations, $P_r(N')$, may be written

$$P_r(N') = P_{r,R}(N') + P_{r,Q}(N') = P_{r,R}(N') + \lambda(N')P_{r,R}(N')$$

where $\lambda(N')$ are the relative A″/A′ λ-doublet populations, and $P_{r,I}(N')$ are the reactive populations obtained using I ≡ R↑ or Q↑ branch data, which probe the A′ and A″ λ-doublet levels, respectively. For the reaction, we have used the population ratios either from our own measurements,[24,42] from Wolfrum and coworkers,[12,13,15,43] or from Zare and coworkers.[41] The λ-doublet population ratios generated in the photodissociation of water were taken from refs. 37, 38 and 44. Note that for the OH formed in the reaction, the A′ λ-doublet levels are the most populated, while for the photolysis of water *via* the $\tilde{A}$ state it is the A″ level which dominates. Thus, only using R↑ data to obtain the relative populations leads to an overestimation of the reaction cross-section. Once averaged over N', we find that the correction factor obtained for the H + H_2O reaction cross-section at 2.46 eV is 0.77, while those for H + D_2O are 0.70 and 0.65 at 1.8 eV and 2.5 eV, respectively. These correction factors are quite modest, and introduce little additional uncertainty into the analysis.

C. Theory

The methodology used in the QCT calculations is essentially the same as that described in previous studies.[7,24,27,29,45] All the calculations were performed on the YZCL2 PES,[22] which has been extended previously for use at higher collision energies.[24] A batch of 2×10^5 trajectories with a maximum impact parameter b_{max} = 1.7 Å was run at collision energy E_t = 2.45 eV for the H + H_2O reaction. For the + D_2O reaction, batches of 2.5×10^4 and 4×10^5 trajectories were run at E_t = 1.8 eV and E_t = 2.5 eV, respectively, using b_{max} = 1.5 Å. The initial distance from the H atom to the $H_2O(D_2O)$ molecule was 8 Å. The ground vibrational state of the rotationless H_2O or D_2O reagent was determined by means of a vibrational action calculation,[46] where actions were converged to 0.05 $\hbar$. Integration of the equations of motion was carried out using an adapted version of the VENUS96 program[47] with a time step of 0.025 fs, which provided a conservation of energy better than 1 in 10^5. The assignment of diatomic product quantum numbers was carried out as in previous works, calculating the rovibrational levels of OH(OD) and H_2(HD) by the semiclassical quantization of the classical action using in each case the asymptotic diatomic potentials of the PES. The classical rotational angular momenta were equated to $[j'(j'+1)]^{1/2}\hbar$. With the (real) j' value so obtained, the vibrational quantum number v' was found by equating the internal energy of the outgoing molecule to the corresponding rovibrational Dunham expansion in $(v'+1/2)$ and $j'(j'+1)$, whose coefficients are calculated by fitting the semiclassical rovibrational energies. The values of v' and j' found in this way were then rounded to the nearest integer.

In previous QCT calculations for this reaction on the WSLFH PES by Schatz and co-workers,[23] the integral cross-sections were calculated by requiring the H_2 product to have at least its zero-point energy. To that effect, those trajectories producing H_2 with internal energy below the zero point were simply discarded. Using this zero-point energy constraint the calculated cross-sections were found to be lower, in better agreement with the time-dependent QM 6D centrifugal sudden calculations carried out on the YZCL1 PES.[18] If no zero-point energy constraints were applied then the cross-sections were too large, and if the zero-point energy of both OH(OD) and H_2(HD) or of just OH(OD) were constrained then the calculated cross-sections were extremely small. However, this procedure is somewhat arbitrary since it is applied only to one of the products of the reaction. Moreover, the time-dependent QM calculations of ref. 18 were performed on a different PES and using the centrifugal sudden approximation, which has proved later to underestimate the integral cross-sections.[25,26]

In the present QCT calculations, we have also found that most trajectories emerge with the OH(OD) vibrational action well below its zero-point energy, whereas this tendency is not so clear for H_2(HD). In order to account for the zero-point energy problem, we have implemented a Gaussian-weighted binning (GB) procedure, similar to that presented in previous work[48] and equivalent to the method proposed by Bonnet and Rayez some years ago.[49] This method consists of weighting the trajectories using a Gaussian function of a given width centered at the quantal action of the product diatom, in such a way that the closer the vibrational action of a given trajectory to the quantal value, the larger the weighting coefficient for that trajectory. In the present case, this procedure has been applied simultaneously to both diatomic product molecules. If w_i (v_{OH}) and w_i (v_{H_2}) are the Gaussian weights of the ith trajectory with OH and H_2 vibrational quantum numbers v_{OH} and v_{H_2}, respectively, then the total integral cross-section is given by

$$\sigma = \frac{\pi b_{max}^2}{N_{tot}} \sum_{i}^{N_r} \sum_{v_{OH}} \sum_{v_{H_2}} w_i(v_{OH}) w_i(v_{H_2}) \qquad (7)$$

where b_{max} is the maximum impact parameter and N_{tot} and N_r are the total number of trajectories and the number of reactive trajectories, respectively.

In the present work we have used a full-width-half-maximum (FWHM) for the Gaussian functions of 0.1. As it will be shown below, the net effect of the application of this binning method for the title reaction is to reduce the total cross-section by ≈25%.

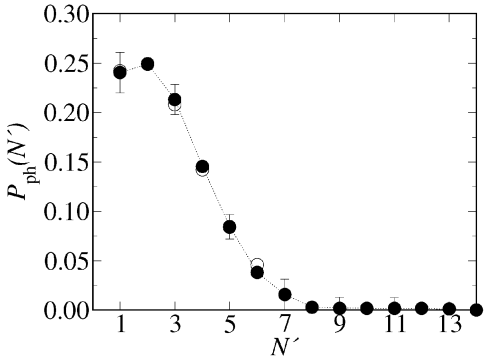

Fig. 2 (●) The OH($v' = 0$) rotational quantum state populations obtained in the present study for the photodissociation of H_2O at 193 nm, compared with those obtained in the previous work (○) of Andresen and coworkers.[44] Both sets of data have been averaged over OH spin-orbit and λ-doublet levels.

III. Results

A. H + H_2O at 2.5 eV

In our previous work on the H + H_2O reaction cross-section[27] we presented OH rotational quantum state population data, $P_{obs}(N')$, obtained under conditions of low [HBr] and high [HBr], together with the fits to the data using the procedures described in Section IIB. We also showed the separate contributions to the signal from reaction and photolysis derived from the fits. At low [HBr] the majority of the OH signal comes from photolysis of water, and leads to a cold rotational quantum state population distribution, while high [HBr] ensures that the majority of the OH signal is generated by reaction, and the OH populations are found to be considerably hotter. The OH rotational quantum state populations observed here for the photodissociation of pure H_2O agree very well with the previous room temperature measurements of Andresen and coworkers,[44] as demonstrated by the comparison shown in Fig. 2. Colder photofragment distributions were obtained in the work of Nesbitt and coworkers,[37] whose experiments were performed under jet cooled conditions. It is known that at room temperature, a significant fraction of the OH photofragment rotational excitation comes from thermal rotational motion in the parent water molecule.[42,44,60] The experimental OH population distribution for reaction (1) is shown in Fig. 3. As seen, very good agreement is obtained with the rotational distribution determined previously by Wolfrum and coworkers.[12] In our previous work we have demonstrated that the population data are also in excellent agreement with the results of both the 5D QM and full-dimensionality QCT calculations employing the YZCL2 PES.[27]

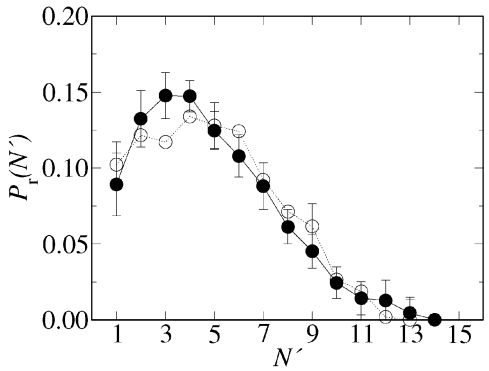

Fig. 3 (●) OH($v' = 0$) rotational quantum state populations generated by the H + H_2O abstraction reaction at 2.46 eV, averaged over spin-orbit and λ-doublet level. (○) Previous experimental data obtained by the group of Wolfrum and coworkers under similar experimental conditions.[13]

Table 1 Cross-section(in Å^2) for the H + H_2O abstraction reaction (1) at collision energies close to 2.46 eV (see also Fig. 4)

Experiment	This work	0.041 ± 0.018
Experiment	[12]	0.26 ± 0.09
5D QM(YZCL2 PES)	[27]	0.10
QCT(YZCL2 PES)[a]	[27]	0.089 ± 0.002
QCT(YZCL2 PES)[b]	[27]	0.067 ± 0.003

[a] Normal binning. [b] Gaussian binning.

The results of the cross-section measurements at 2.46 eV are presented in Table 1 and Fig. 4. For completeness, we note that Schatz and coworkers[23] obtained a value of 0.0933 ± 0.0052 Å^2 in their H_2 zero point energy corrected QCT calculations on the WSLFH PES (see preceding section). As noted previously,[27] the abstraction reaction cross-section we obtain here is significantly smaller than the previous estimates of Wolfrum and Kleinermanns and coworkers[11–13,16,17] (see further discussion in Section IV), the present measurement being in better agreement with the theoretical determinations. It should be mentioned that there have been two recent determinations of the H_2O absorption cross-section at 193 nm which were not included in the evaluation of the recommended absorption cross-section data that we have used.[33] Because the photodissociation of H_2O is the calibrant for the reaction cross-section, errors in its absorption cross-section will directly map onto errors in our estimate of the reaction cross-section (see eqn. (3)). The new absorption cross-section measurements are from the work of Chung *et al.*[35] and Parkinson and Yoshimo.[36] The values they obtain, $\sigma_{H_2O} = 1.62 \times 10^{-21}$ cm^2,[35] and 1.92×10^{-21} cm^2,[36] straddle the recommended value, and thus it is unlikely that significant errors in our reaction cross-section arise from errors in the cross-section of the photolytic precursor employed as the calibrant.

B. H + D_2O at 1.8 eV and 2.5 eV

Examples of the raw OD populations derived from the experiments, together with the fits to the data, are shown in Fig. 5 at the two collision energies studied. Notice that at 2.5 eV the photolytic contribution to the signal is quite small, while at 1.8 eV, it is the reactive signal which represents a minor contribution, reflecting the twenty-fold decrease in the photodissociation cross-section for the H-atom precursors HBr and HCl. The photofragment OD rotational population distribution determined for photolysis of mixtures of D_2O and HOD at

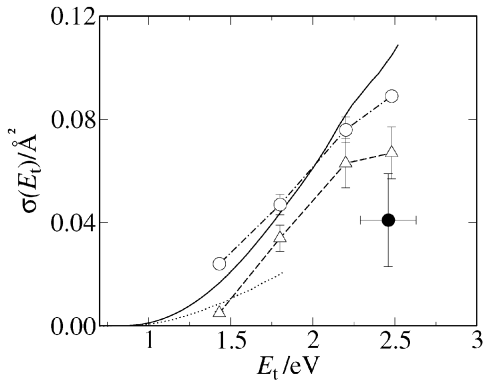

Fig. 4 Comparison between the experimental abstraction reaction cross-section for the H + H_2O reaction (● with error bars), and 5D QM calculations using the YZCL2 PES (—).[27] The 'error bar' in E_t on the experimental cross-section allows for the possibility of translational cooling at high values of $p\Delta\tau$ (see Section IV). The 6D QM cross-sections (···),[18] which employed the CS approximation together with the YZCL1 PES, and the QCT data using normal (○) and Gaussian (△) binning procedures and the YZCL2 PES are also shown (see text for details).

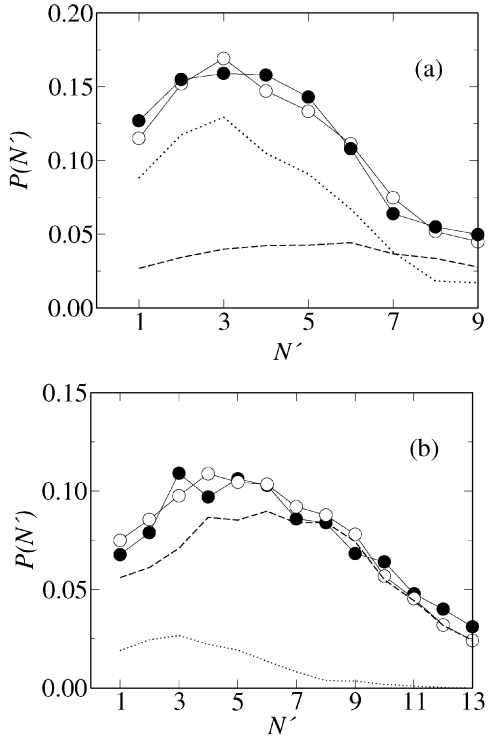

Fig. 5 Example raw OD($v' = 0$) rotational quantum state populations (●), together with the fits to the population data (○) recorded at (a) 1.83 eV and (b) 2.48 eV. The lines without symbols show the results of the fits: ··· the HOD/D_2O photolysis contribution to the signal, where the photolysis populations were obtained in separate experiments without HCl or HBr present; -- the reactive contribution to the signal, where the reactive populations are taken from the literature, as described fully in Section IIB.

193 nm is shown in Fig. 6. In the analysis we have assumed that the two molecules yield the same OD rotational population distributions, in agreement with the previous findings of Nesbitt and coworkers.[38] As noted already, our OD photofragment rotational distribution is hotter than observed in the jet-cooled experiments,[37,38] because some of the rotational motion in the warm parent molecule is transferred to the OD photofragment. This effect is quantitatively accounted for in the Franck–Condon model developed by Balint-Kurti.[50] The OD population distribution calculated using this model, assuming a rotational temperature of 300 K for D_2O, has been calculated previously,[42] and is shown in Fig. 6 for comparison.

The abstraction reaction cross-sections for the H + D_2O reaction at the two collision energies studied are compared with the previous experimental results by Wolfrum and cow-

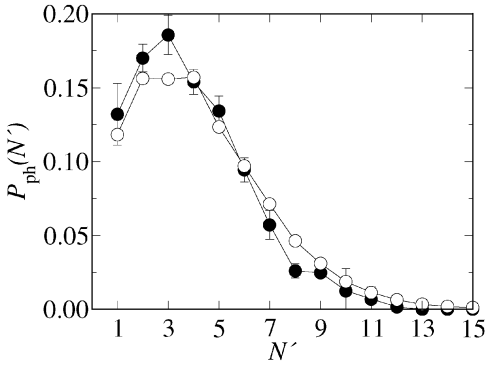

Fig. 6 (●) OD($v' = 0$) rotational quantum state populations for the photodissociation of D_2O at 193 nm derived from the present experiments without HCl or HBr present. The data are compared with the results of Franck–Condon model calculations described in the text (○)[50] and reported previously in ref. 42.

Table 2 Cross-section(in Å^2) for the abstraction reaction H + D_2O at mean collision energies close to 1.8 eV and 2.46 eV

	$\langle E_t \rangle$	1.8 eV	2.5 eV
Experiment	This work	0.0056 ± 0.0019	0.0087 ± 0.0034
Experiment	14,15	0.10 ± 0.03	0.11 ± 0.02
6D QM(YZCL1)[a]	18	0.0053	0.010
QCT(YZCL2 PES)	This work[b]	0.009 ± 0.001	0.030 ± 0.003
QCT(YZCL2 PES)	This work[c]	0.005 ± 0.001	0.022 ± 0.003

[a] Employing the CS approximation. [b] Normal binning. [c] Gaussian binning.

orkers[14,15] and the QCT results on the YZCL2 PES in Table 2 and Fig. 7. For comparison, Schatz and coworkers[23] obtained 0.0074 ± 0.0005 Å^2 and 0.0105 ± 0.0005 Å^2 at collision energies of 1.8 eV and 2.6 eV, respectively, employing QCT methods on the WSLFH PES, and neglecting trajectories with H_2 internal energies below the zero point energy (see Section IIC). As with the results for the H + H_2O reaction, there is a large discrepancy between the experimental results presented here, and the previous experimental cross-section determinations by Wolfrum and coworkers.[14,15] Note, however, that the new data agree better with the QCT calculations, particularly if the latter employ the Gaussian-weighted binning procedure (see Fig. 7).

As noted in the preceding subsection, Chung *et al.* have recently determined the absorption cross-sections for H_2O and its isotopomers at 295 K, a temperature close to that used in the present measurements.[35] Their absorption cross-section values for HOD and D_2O, *relative* to that for H_2O, are 0.315 and 0.099, respectively. By summing over the two photolysis channels of DOH/HOD, the corresponding jet-cooled photodissociation data of Nesbitt and coworkers,[37,38] used in the present work, are 0.424 and 0.0157. Thus, while the relative absorption cross-sections for HOD from the two experiments seem in reasonable agreement, the relative cross-sections for D_2O differ by about a factor of six. It is unclear whether or not this difference in data reflects a genuine difference in the absorption cross-section of water and its isotopomers at the temperatures employed in the two studies, or is a result of (very minor) isotopic impurities. Unlike the study by Chung *et al.*,[35] the possibility of isotopic contamination could be very carefully monitored in the work of Nesbitt and coworkers,[38] because they directly observed the OH and OD photofragments by LIF. Nevertheless, to test the sensitivity of our H + D_2O reaction cross-section, we have refitted the population data employing the absorption cross-sections of Chung *et al.* We have had to assume that for DOH/HOD the branching ratio for dissociation into OH and OD is the same as that determined by Nesbitt and coworkers,[38] since this quantity was not determined in the experiments of Chung *et al.* The H +

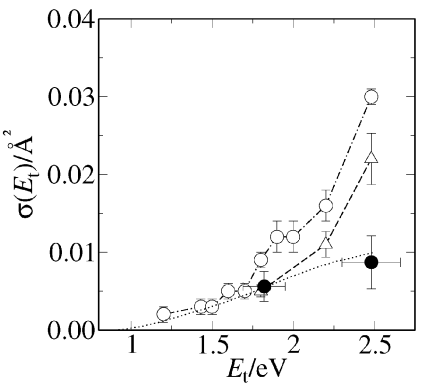

Fig. 7 As for Fig. 4, but showing the cross-sections for the H + D_2O abstraction reaction.

D_2O abstraction reaction cross-sections are increased by factors of 2.4 and 2.6 at the collision energies of 1.8 eV and 2.5 eV, respectively, if the Chung *et al.*[35] data are employed. The reason that the increase in reactive cross-section is not larger, *i.e.* closer to a factor of six, is because, under the conditions employed, the majority of the photolytic OD signal comes from the photodissociation of HOD, irrespective of which set of absorption cross-section data are assumed. Furthermore, the two studies are in reasonable agreement about the relative absorption cross-section of HOD.

IV. Discussion

As noted above, our experimentally determined cross-sections for the H + H_2O and H + D_2O abstraction reactions are about an order of magnitude smaller than the previous determinations by Wolfrum and Kleinermanns and their coworkers at similar collision energies.[11–16] While we have taken special care to eliminate possible sources of error in our experiments, perhaps the most convincing evidence in support of the present data is that competitive photodissociation of H_2O was also observed in the second set of experiments at 193 nm reported by Wolfrum and coworkers.[12] This observation, like our own, places a constraint on the abstraction reaction cross-section relative to the absorption cross-section of H_2O. Given that it is unlikely that the absorption cross-section of the H_2O calibrant employed here is in error by a factor of ten,[33,34] our conclusion is that difficulties may have arisen in the previous abstraction cross-section measurements[11–13,16] due to the use of separate, highly reactive, photolytic calibrants with absorption cross-sections between 10 and 500 times that of water at 193 nm.

There are a number of potential complications with the cross-section measurements, common to both the present work and that of Wolfrum and Kleinermanns and their coworkers,[11–16] which should be considered. A factor not previously considered is the possibility that the HX photolysis precursor may be depleted, or completed removed, by photodissociation. If removed completely, the Beer–Lambert law calculation would potentially lead to an overestimate of the H-atom reactant number density, and a consequent underestimate of the reaction cross-section. Note that depletion of the H-atom precursor by photolysis is more likely to be an issue with HBr than with HCl, because of its twenty-fold higher absorption cross-section. Nevertheless, even for HBr, we estimate that, with the 193 nm pulse energies employed here ($\lesssim$25 mJ cm^{-2}, entering the reaction chamber), less than 10% of the HBr precursor is photolyzed per laser shot. It seems unlikely, therefore, that photolytically removal of HBr can account for the factor-of-two discrepancy between theory and experiment observed here at a collision energy of 2.5 eV.

The foregoing treatment of the experimental data, in common with the original work by Wolfrum and Kleinermanns and coworkers,[11–16] also assumes that H atoms are not removed significantly on the laser pump–probe timescales employed. The most likely removal pathways for H are abstraction reactions with the target H_2O reactant or the competing reaction with the HX precursor, for example,

$$H + HBr \rightarrow H_2 + Br \qquad (8)$$

The cross-section for this reaction has been determined by Valentini and coworkers to be 3($\pm$1) Å^2,[51] apparently nearly two orders of magnitude larger than for the H + H_2O abstraction reaction. However, their determination of the cross-section of the H atom abstraction reaction with HCl is about ten times larger than the most recent determinations by Volpp and Wolfrum and coworkers.[52–54] Nevertheless, if we assume the larger value for this reaction cross-section, only 4% of hot H atoms react with HBr within a 50 ns timescale, and 12% within a 150 ns timescale. It seems that the abstraction reactions of H with the HX precursor, or with H_2O, cannot be responsible for significant H atom loss in the present experiments.

Scattering of the hot H atoms, either with the precursor HX, or with the target H_2O, may also take place *via* alternative pathways such as

$$H + HBr \rightarrow H + HBr^* \qquad (9)$$

Processes of this type lead to translational cooling of the H atoms, rather than to their removal, and include both the exchange reactions, as well as inelastic scattering, probably the dominant process. Translational moderation of the H atoms should also be included under this heading, but the large mass difference between the H atoms and the target or precursor molecules render this process very inefficient. QCT calculations for the H + HCl reaction,[53] as well as experimental measurements by Polanyi and coworkers,[55] suggest cross-sections for the H + HX exchange reaction of $\sim$1 Å^2, similar in magnitude to the H atom exchange reaction with water.[7,18,25] The total cross-section for process (9) (*i.e.* inelastic scattering plus exchange) has been estimated to be 11 $\pm$ 2 Å^2,[56] and varies little with the nature of X. Somewhat smaller cross-sections ($\sim$3 Å^2) have been calculated using QCT methods by Kudla and Schatz[57] for inelastic scattering of H with H_2O. Process (2), in common with the reactions of H with the HCl and HI, leads to rather inefficient H-atom translational to HX vibrational or rotational excitation,[56] with only 10–15% of the energy transferred per collision. Assuming 10% cooling per collision, it can be estimated that, at the pressures used in the present study, only 3% to 12% cooling of the H atoms will occur between 50 ns and 200 ns. This estimate is supported by the direct measurements by Wolfrum and coworkers[17] of H atom Doppler resolved profiles as a function of time delay, in mixtures of between 50 and 150 mTorr H_2S, 120 mTorr D_2O, and 1.4 Torr Ar. Even under these relatively high pressure conditions, compared to those employed in the present work, these measurements indicate only modest cooling on the 100 ns timescale. The *x*-axis error bars placed on the experimental data of Figs. 4 and 7 provide an indication of the maximum extent of translational cooling that we would expect under the condtions used here.

We have reported previously on the good agreement between QCT and QM calculated abstraction cross-sections for the H atom reaction with H_2O[27] (shown in Tables 1 and 2 and Figs. 4 and 7). This result is perhaps not surprising given previous theoretical work on the direct H + H_2 abstraction reaction.[58] The calculated cross-sections employing the YZCL2 PES are about a factor of 2 to 3 larger than the present experimental values. It is possible that the PES is insufficiently accurate in the high energy region relevant to the abstraction reaction. However, the fact that the QCT calculations by Schatz and coworkers[23] yield cross-sections of similar magnitude to those reported here for both the H + H_2O and H + D_2O reactions might be taken as evidence that errors in the ground state PES are not responsible for the discrepancy. A further complication to the dynamics is that an excited electronic state may play a role at the energies sampled by the experiments: High level *ab initio* calculations [QCISD(T)/aug-cc-pVTZ] show that, at the saddle point configuration for reaction (1), the lowest excited state has an electronic energy only $\sim$2 eV above the equilibrium energy of the reactants. Therefore, it is possible that this excited state could influence the reaction cross-section at 2.46 eV. In this context, it is perhaps significant that the experimental abstraction reaction cross-section for H + D_2O at 1.8 eV is in much better agreement with theory than the data at 2.5 eV.

Further difficulties may arise with the approximations used in the dynamical calculations. As noted in the introduction, although the 6D QM calculations employing the YZCL1 PES[18] appear to be in excellent agreement with the present

$H + H_2O$ and $H + D_2O$ experiments, they employ the CS approximation, which is now known to be unreliable for this reaction.[26] The 5D QM calculations, on the other hand, treat rotation rigorously,[27] but freeze the spectator OH bond. While this appears to be an excellent assumption up to energies around 1.5 eV,[25] it may be less reliable at the high energy employed here. As commented on in Section IIC, the present QCT calculations reveal that most trajectories emerge with the OH vibrational action below its zero-point energy. When trajectories are weighted with a Gaussian function centered on the OH quantum mechanical vibrational action, rather than binned in the conventional way, the reaction cross-section is reduced to 0.067 $Å^2$, in somewhat better agreement with experiment (see Fig. 4). By contrast, the Gaussian-weighted binning applied only to the H_2 fragment has little effect on the cross-section. A further assumption in the dynamical calculations is the neglect of rotation in the H_2O reactant. It has been found classically for this reaction that including reagent rotation increases the cross-section,[20,23,29] but at 300 K only by a modest amount. Quantum mechanically, the effect of H_2O rotation would have to be in the opposite sense to, and significantly more pronounced than, that predicted classically to bring theory and experiment into better agreement.

The effect of isotopic substitution on the integral cross-section provides interesting comparisons between the various dynamical calculations, and the potential energy surfaces they employ. Comparison between the experimentally determined isotope effect and those determined by theory is shown in Fig. 8. We attribute the fact that abstraction of H is faster than abstraction of D principally to the zero-point energy differences in the initial state, which increase the effective barrier for $H + D_2O$ relative to that for $H + H_2O$. An additional effect may be due to the more efficient transfer of collision energy from the H atom to the lighter H_2O molecule as compared with D_2O. It was found that this effect was the main reason for the larger cross-sections of the $D + H_2$ reaction with respect to those for $H + D_2$.[60] Tunnelling may also play some role at low collision energies in promoting H-atom abstraction. Aside from this, the vibrational motion of the D_2O reactant samples a smaller range of displacements compared with that for H_2O, thereby restricting the cone of acceptance in the deuterated reaction. At 1.5 eV this effect has been observed to be reflected in the differential cross-sections for the $H + H_2O$ and $H + D_2O$ reactions, which tend to be significantly more backward scattered in the latter case.[42] While the experimental errors are large in the present experiments, the data appear to be sufficiently precise to distinguish between the QCT calculations on the OC,[61] the WSLFH (not shown),[23] and the YZCL2 PESs.[27] Interestingly, the collision energy dependence of the kinetic isotope effect predicted by the alternative calculations is remarkably different. The experiments from this work, together with those from the groups of Zare and coworkers[41] and Wolfrum and coworkers,[17] seem to indicate a modest increase in isotope effect with increasing collision energy, which is at variance with the QCT calculations presented here on the YZCL2 PES.

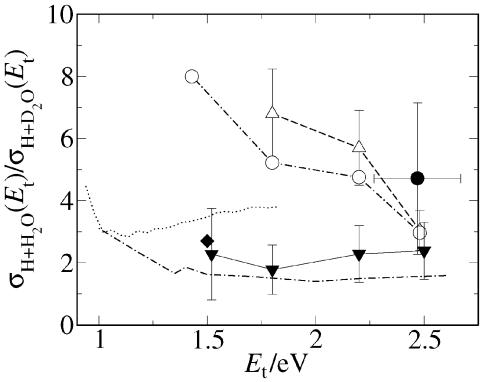

Fig. 8 Comparison between the experimental and calculated abstraction reaction isotope effects. Present experimental result: (●) with error bars; 6D QM calculations on the YZCL1 PES (···)[18] which employed the CS approximation; Present QCT calculations using the YZCL2 PES with normal (○) and Gaussian (Δ) binning; (--) QCT calculations on the OC PES;[61] (▼) experimental data from Wolfrum and coworkers, taken from ref. 17 (◆) experimental data of Zare and coworkers.[41]

V. Conclusions

We have presented determinations of the abstraction reaction cross-sections for $H + H_2O$ and $H + D_2O$. The data are compared with previously published 5D QM scattering calculations and new full dimensionality QCT calculations using the most recent YZCL2 PES. The calculated absolute cross-sections and OH/OD rotational quantum state distributions are compared with new experimental results obtained at mean collision energies around 1.8 eV and 2.5 eV. The new experimental cross-sections are in much better agreement with the theoretical data than previous experimental studies. However, particularly at the higher collision energy there remains a factor of two discrepancy between theory and experiment for the abstraction reaction cross-section, the origin of which is unclear at present. The experimental isotope effect at 2.5 eV is in reasonable agreement with the new QCT calculations, although the latter seem to show a different collision energy dependence that that displayed by the combined experimental data set from this work, and previous studies of Zare[41] and Wolfrum and their coworkers.[17]

Acknowledgements

The following support is gratefully acknowledged: the Royal Society of London, EPSRC, and SSF (for grants to M.B., and to S.M.); the "Ramón y Cajal" programme of the Spanish Ministry of Science and Technology (for J.F.C.). The Spanish work has been financed by DGES (Project BQU2002-04627-C02-02). The work is also supported in part by the European Community's Human Potential Programme under Contract HPRN-CT-1999-00007, *Reaction Dynamics*. L. Rubio Lago and S. Marinakis acknowledge the financial support provided through the same European Community's Programme.

References

1 J. M. Bowman and G. C. Schatz, *Annu. Rev. Phys. Chem.*, 1995, **46**, 169.
2 D. C. Clary, *Science*, 1998, **279**, 1879.
3 (*a*) P. Casavecchia, N. Balucani and G. G. Volpi, *Annu. Rev. Phys. Chem.*, 1999, **50**, 347; (*b*) P. Casavecchia, *Rep. Prog. Phys.*, 2000, **63**, 355.
4 G. C. Schatz, *Science*, 2000, **290**, 950.
5 J. J. Valentini, *Ann. Rev. Phys. Chem.*, 2001, **52**, 15.
6 I. W. M. Smith and F. F. Crim, *Phys. Chem. Chem. Phys.*, 2002, **4**, 3543, and references therein.
7 J. F. Castillo, *ChemPhysChem*, 2002, **3**, 320.
8 M. Brouard, P. O'Keeffe and C. Vallance, *J. Phys. Chem. A*, 2002, **106**, 3629.
9 J. N. Bradley, *Flame and Combustion Phenomena*, Methuen, London, 1969, p. 77.
10 J. V. Michael and J. W. Sutherland, *J. Phys. Chem.*, 1988, **92**, 3853 and references therein.
11 K. Kleinermanns and J. Wolfrum, *Appl. Phys. B*, 1984, **34**, 5.
12 A. Jacobs, H.-R. Volpp and J. Wolfrum, *24th International Symposium on Combustion*, The Combustion Institute, Pittsburgh, PA, 1992, 605.
13 A. Jacobs, H.-R. Volpp and J. Wolfrum, *J. Chem. Phys.*, 1994, **100**, 1936.
14 A. Jacobs, H.-R. Volpp and J. Wolfrum, *Chem. Phys. Lett.*, 1996, **196**, 249.

15 S. Koppe, T. Laurent, P. D. Naik, H.-R. Volpp and J. Wolfrum, *Can. J. Chem.*, 1994, **72**, 615.
16 K. Kessler and K. Kleinermanns, *Chem. Phys. Lett.*, 1992, **190**, 145.
17 H. Szichman, M. Baer, H.-R. Volpp and J. Wolfrum, *J. Phys. Chem.*, 1999, **111**, 567.
18 D. H. Zhang, M. A. Collins and S.-Y. Lee, *Science*, 2000, **290** 961.
19 D. H. Zhang, D. Xie, M. Yang and S.-Y. Lee, *Phys. Rev. Lett.*, 2002, **89**, 283203.
20 (*a*) G. Wu, G. C. Schatz, G. Lendvay, D.-C. Fang and L. B. Harding, *J. Chem. Phys.*, 2000, **113**, 3150; (*b*) G. Wu, G. C. Schatz, G. Lendvay, D.-C. Fang and L. B. Harding, *J. Chem. Phys.*, 2000, 7712.
21 (*a*) M. J. T. Jordan and M. A. Collins, *J. Chem. Phys.*, 1996, **104**, 4600; (*b*) R. P. A. Bettens, M. A. Collins, M. J. T. Jordan and D. H. Zhang, *J. Chem. Phys.*, 2000, **112**, 10162.
22 (*a*) M. Yang, D. H. Zhang, M. A. Collins and S.-Y. Lee, *J. Chem. Phys.*, 2001, **114**, 4759; (*b*) M. Yang, D. H. Zhang, M. A. Collins and S.-Y. Lee, *J. Chem. Phys.*, 2001, **115**, 174.
23 D. Troya, M. Gonzalez and G. C. Schatz, *J. Chem. Phys.*, 2001, **114**, 8397.
24 M. Brouard, I. Burak, D. Minayev, P. O'Keeffe, C. Vallance, F. J. Aoiz, L. Bañares, J. F. Castillo, D.H. Zhang and M. A. Collins, *J. Chem. Phys.*, 2003, **118**, 1162.
25 D. H. Zhang, M. Yang and S.-Y. Lee, *Phys. Rev. Lett.*, 2002, **89**, article 103201.
26 D. H. Zhang, M. Yang and S.-Y. Lee, *J. Chem. Phys.*, 2002, **117**, 10067.
27 M. Brouard, I. Burak, S. Marinakis, D. Minayev, P. O'Keeffe, C. Vallance, F. J. Aoiz, L. Bañares, J. F. Castillo, D. H. Zhang, D. Xie, M. Yang, S. Lee and M. A. Collins, *Phys. Rev. Lett.*, 2003, **90**, 93201.
28 (*a*) J. Ischtwan and M. A. Collins, *J. Chem. Phys.*, 1994, **100**, 8080; (*b*) M. J. T. Jordan, K. C. Thompson and M. A. Collins, *J. Chem. Phys.*, 1995, **102**, 5647.
29 J. F. Castillo, F. J. Aoiz and L. Bañares, *Chem. Phys. Lett.*, 2002, **356**, 102.
30 J. Luque and D. R. Crosley, *LIFBASE: Database and simulation program v. 1.6., SRI International Report MP 99-009*, 1999.
31 B. J. Huebert and R. M. Martin, *J. Phys. Chem.*, 1968, **72**, 3046.
32 J. B. Nee, M. Suto and L. C. Lee, *J. Chem. Phys.*, 1986, **85**, 4919.
33 R. Atkinson, D. L. Baulch, R. A. Cox, J. N. Crowley, R. F. Hampson, Jr., J. A. Kerr, M. J. Rossi and J. Troe, *J. Phys. Chem. Ref. Data*, 2000, **29**, 167, and references to earlier evaluations therein.
34 C. A. Cantrell, A. Zimmer and G. S. Tyndall, *Geophys. Res. Lett.*, 1997, **24**, 2195.
35 C. Y. Chung, E. P. Chew, B. M. Cheng, M. Bahou and Y. P. Lee, *Nucl. Instrum. Methods Phys. Res., Sect. A*, 2001, **467**, 1572.
36 W. H. Parkinson and K. Yoshimo, *Chem. Phys.*, 2003, **294**, 31.
37 D. F. Plusquellic, O. Votava and D. J. Nesbitt, *J. Chem. Phys.*, 1997, **107**, 6123.
38 D. F. Plusquellic, O. Votava and D. J. Nesbitt, *J. Chem. Phys.*, 1998, **109**, 6631.
39 (*a*) J. W. Pyper, R. S. Newbury and G. W. Barton, *J. Chem. Phys.*, 1967, **46**, 2253; (*b*) J. W. Pyper and L. D. Christensen, *J. Chem. Phys.*, 1975, **62**, 2596.
40 M. Bahou, C.-Y. Chung, Y. P. Lee, B.-M. Cheng, Y. L. Yung and L. C. Lee, *Astrophys. J.*, 2001, **559**(Part 2), L179.
41 M. J. Bronikowski, W. R. Simpson and R. N. Zare, *J. Phys. Chem.*, 1993, **97**, 2194.
42 M. Brouard, I. Burak, D. M. Joseph, G. A. J. Markillie, D. Minayev, P. O'Keeffe and C. Vallance, *J. Chem. Phys.*, 2001, **114**, 6690.
43 A. Jacobs, H.-R. Volpp and J. Wolfrum, *Chem. Phys. Lett.*, 1994, **218**, 51.
44 D. Hausler, P. Andresen and R. Schinke, *J. Chem. Phys.*, 1987, **87**, 3949.
45 J. F. Castillo, F. J. Aoiz, L. Bañares and J. Santamaria, *Chem. Phys. Lett.*, 2000, **329**, 517.
46 C. W. Eaker and G. C. Schatz, *J. Chem. Phys.*, 1984, **81**, 2394.
47 W. L. Hase *et al.*, *QCPE*, 1996, **16**, 671.
48 L. Bañares, F. J. Aoiz, P. Honvault, B. Bussery-Honvault and J. -M. Launay, *J. Chem. Phys.*, 2003, **118**, 565.
49 L. Bonnet and J. C. Rayez, *Chem. Phys. Lett.*, 1997, **277**, 183.
50 G. G. Balint-Kurti, *J. Chem. Phys.*, 1986, **84**, 4443.
51 P. M. Aker, G. J. Germann and J. J. Valentini, *J. Chem. Phys.*, 1989, **90**, 4795.
52 R. A. Brownsword, C. Kappel, P. Schmiechen, H. P. Upadhyaya and H.-R. Volpp, *Chem. Phys. Lett.*, 1998, **289**, 241.
53 F. J. Aoiz, L. Banares, T. Bohm, A. Hanf, V. J. Herrero, K.-H. Jung, A. Lauter, K. W. Lee, M. Menendez, V. Saez Rabanos, I. Tanarro, H.-R. Volpp and J. Wolfrum, *J. Phys. Chem. A*, 2000, **104**, 10452.
54 A. Hanf, A. Lauter, D. Suresh, H.-R. Volpp and J. Wolfrum, *Chem. Phys. Lett.*, 2001, **340**, 71.
55 V. J. Barclay, B. A. Collings, J. C. Polanyi and J. H. Wang, *J. Phys. Chem.*, 1991, **95**, 2921.
56 P. M. Aker, G. J. Germann, K. D. Tabor and J. J. Valentini, *J. Chem. Phys.*, 1989, **90**, 4809.
57 K. Kudla and G. C. Schatz, *J. Chem. Phys.*, 1993, **98**, 4644.
58 F. J. Aoiz, L. Banares and V. J. Herrero, *J. Chem. Soc. Faraday Trans.*, 1998, **94**, 2483, and references therein.
59 M. Brouard, S. Langford and D. E. Manolopoulos, *J. Chem. Phys.*, 1994, **101**, 7458.
60 F. J. Aoiz, L. Banares, V. J. Herrero, V. Sáez Rábanos and I. Tanarro, *J. Phys. Chem. A*, 1997, **101**, 6165.
61 J. F. Castillo and J. Santamaría, *J. Phys. Chem. A*, 2000, **104**, 10414.